



Sensitivity of the MAECHAM4 model to imposed ozone distributions

*Anne Grete Straume, Elisa Manzini and
Peter Siegmund*

Intern rapport; IR 2002-02

De Bilt, 2002

PO Box 201
3730 AE De Bilt
Wilhelminalaan 10
De Bilt
The Netherlands
Telephone +31(0)30-220 69 11
Telefax +31(0)30-221 04 07

Auteurs: A.G. Straume, E. Manzini, P. Siegmund

De reeks *Intern rapport* is in juli 2000 gestart en geeft bij afsluiting de vorderingen rond een project of instrument weer. De inhoud is primair bestemd voor KNMI'ers, maar de publicaties zijn verder openbaar. Lezers van buiten het instituut dienen er echter wel rekening mee te houden dat het gebruikte jargon niet in alle gevallen voor buitenstaanders duidelijk zal zijn.

Sensitivity of the MAECHAM4 model to imposed ozone distributions

Anne Grete Straume^{1,3}, Elisa Manzini², and Peter Siegmund¹

¹Royal Netherlands Meteorological Institute (KNMI), De Bilt, The Netherlands

²Max-Planck-Institute for Meteorology, Hamburg, Germany

³Now at: Space Research Organization Netherlands (SRON), Utrecht, The Netherlands

Abstract

Two climate model runs have been performed with the middle atmosphere general circulation model MAECHAM4, using different ozone distributions. This was done to evaluate the model's sensitivity, including its radiative and dynamical responses, to ozone changes in the atmosphere. The first ozone distribution was calculated by a 2-dimensional chemical model at the MPI-Mainz (the MAINZ ozone distribution). The second ozone distribution was compiled at the KNMI from ozone sonde and satellite data over the period 1980 to 1990 (the KNMI ozone climatology). The differences in ozone are small in the troposphere. The largest differences are found in the lower stratosphere with 20% lower ozone concentrations for the KNMI ozone climatology in the tropics, and between 40% and 300% lower ozone concentrations over the poles. In the upper stratosphere, the ozone concentrations are instead -20% higher for the KNMI ozone climatology. These ozone differences lead to changes in the stratospheric and mesospheric temperatures on the order of 2 to 8 K, and differences in the zonal winds occur in accordance with the thermal wind relation. The differences in zonal wind are on the order of 2 to 8 m/s. No significant temperature differences were found near the surface. Changes of the circulation furthermore lead to changes in the polar upper stratosphere temperatures in January (North Pole only) and October (both South and North Poles).

1. Introduction

Ozone is an important climate gas: It absorbs both incoming shortwave and outgoing longwave radiation. The vertical distribution of ozone is decisive for the atmospheric temperature profile, which in turn influences the atmospheric general circulation (e.g. Ramanathan *et al.* 1976; Lacis *et al.* 1990; Wang *et al.* 1995). Even though the greenhouse efficiency of tropospheric ozone is larger than that of stratospheric ozone (Wang *et al.* 1980), observed changes in stratospheric ozone have been shown to induce changes in surface temperature as well as changes in the stratospheric temperature and dynamics (eg. Ramaswamy *et al.* 1996). Whereas an increase in ozone concentrations in the troposphere leads to a surface warming, an increase of ozone in the stratosphere will lead to a surface cooling or warming depending on the altitude where the ozone increase occurs (Lacis *et al.* 1990). According to Lacis *et al.* (1990), the introduction of a positive increment of ozone in the troposphere leads to an increased heating of the surface temperature, and the higher up the increment is introduced the larger the effect on the surface heating. This heating response reaches a maximum around the tropopause. In the lower stratosphere the introduction of an ozone increment will still give a surface warming, but the effect decreases with height until about 30 km (~10 hPa) above the surface. Above this altitude an increase in ozone leads to a surface cooling because the cooling effect caused by absorption of incoming solar radiation dominates over the warming effect

caused by absorption of longwave radiation. The maximum concentration of ozone is located at about 10 hPa, i.e. in the lower stratosphere. The shape of the ozone profile and especially the altitude and magnitude of the ozone maximum is therefore important for a correct global circulation model (GCM) simulation of the surface temperature, the dynamics, and for the radiation budget of the atmosphere.

Since 1979, a cooling of the lower stratosphere has been observed. The cooling was significant over the Northern Hemisphere mid latitudes during January - June, and large but not significant over the Polar Regions during March - April. In the Southern Hemisphere, significant cooling took place over the Antarctic during October - November and from 30°S to 50°S during summer (December - April) (Randel and Cobb 1994). The reason for the cooling is believed to be strongly linked to stratospheric ozone depletion and carbon dioxide increase as discussed in several papers, e.g. van Dorland and Fortuin (1994), Randel and Cobb (1994), Bintanja *et al.* (1996), Ramaswamy *et al.* (1996), Solomon (1999), WMO (1999), and Straume *et al.* (1999). Lower stratospheric ozone depletion due to increased halocarbon levels and heterogeneous chemistry was shown to be associated with observed cold Arctic and Antarctic winter and spring temperatures (Solomon 1999). However, the trend and seasonality of ozone depletion at midlatitudes can, according to Fusco and Salby (1999), not be fully explained by the chemical ozone depletion alone. They showed that most of the variation of total ozone in midlatitudes is accounted for by variations in the upwelling planetary wave activity from the troposphere. Other recent studies suggest other mechanisms for the lower stratospheric cooling. Forster and Shine (1999) and Kirk-Davidoff *et al.* (1999) suggested that a strong correlation between stratospheric ozone depletion and cooling in the late winter and spring Arctic vortex is related to increases in stratospheric water vapor forced by rising sea surface temperatures in the tropics. Thompson and Wallace (1998) suggested that the changes in lower stratospheric temperatures over the Arctic are also linked to natural variability in the tropospheric wave activity associated with the Arctic Oscillation.

A few recent studies have used GCMs to study the effect of ozone changes on the temperature distribution and dynamics of the atmosphere. In a study by Ramaswamy *et al.* (1996), observed ozone trends were introduced in the lower stratosphere of a GCM simulation. The observed trends showed lower-stratospheric ozone decreases in both hemispheres on the order of 3% over the period 1979 to 1990. The ozone trends lead, according to Ramaswamy *et al.* (1996), to a global mean temperature decrease in the lower stratosphere on the order of 0.6 K. Extratropical decreases in ozone gave temperature decreases also into the lower tropical stratosphere where no ozone changes took place. The temperature decreases in this region were explained by an increase in upward motion rates with a corresponding increase in adiabatic cooling. Christiansen *et al.* (1997) studied the response of a three-dimensional GCM on imposed changes in the ozone distribution from a 300-days simulation for perpetual January conditions. They found that a uniform 50% reduction of ozone in the lower stratosphere from about 100 to 20 hPa leads to a cooling of the lower stratosphere with a maximum response of -20 K over the tropics and a minimum of -1 K over the poles. In the upper stratosphere, a heating of up to 5 K occurred. Over the North Pole a cooling with a maximum of -15 K occurred in the layer between the lower stratosphere and 1 hPa, due to changes in the meridional circulation. The winter upper stratospheric jet increased in magnitude with 40 m/s, whereas the changes outside the jet were small. The reduction of ozone lead, furthermore, to a weakening of the planetary wave activity. These studies show that changes in ozone in the upper troposphere and lower stratosphere influence not only

the local temperature but also the temperature in other parts of the atmosphere as well as the general circulation.

In the present study two multi-year simulations have been performed with a general circulation model, the middle atmosphere MAECHAM4 model, using two different ozone distributions. The motivation is to evaluate the sensitivity of the GCM climate of the troposphere, stratosphere and mesosphere to the imposed ozone distributions. The ozone distributions used are i) the ozone distribution used in the standard configuration of the MAECHAM4 model and ii) an observation-based ozone climatology compiled at the Royal Netherlands Meteorological Institute (KNMI) (Fortuin and Kelder 1998). Given that the standard MAECHAM4 model ozone distribution is derived from a two-dimensional chemical model (Brühl 1993), an outcome of the comparison of the model responses to the two distributions is the evaluation of the model biases due to the current use of a distribution not based on observations. In addition, the KNMI climatology is going to be the standard climatology to be used in the cycle 5 of the model. The present work therefore serves as a documentation of the developmental changes from die MAECHAM4 to MAECHAM5 models.

2. The General Circulation Model

The MAECHAM4 model is described by Manzini *et al.* (1997). It is the middle atmosphere version of die ECHAM4 general circulation spectral transform model with state-of-the-art physical parameterizations. The ECHAM4 model is described by Roeckner *et al.* (1996). The simulations presented here are performed at T30 (triangular truncation) horizontal resolution. The MAECHAM4 model has 39 levels in the vertical (L39) from the surface up to 0.01 hPa (about 80 km). In the stratosphere, die vertical resolution is about 1.5 km and the resolution decreases slowly up to 6-7 km at the model top in die lower mesosphere. The gravity wave parameterization consists of two parts, separately representing the effects of die momentum deposition from orographic gravity waves and from a continuous and broad gravity wave spectrum arising from a variety of gravity wave sources, as convection, fronts and dynamical instabilities. Sensitivities to the specifications of the gravity wave parameterizations are discussed in Manzini and McFarlane (1998).

3. The Ozone Distributions

The first ozone distribution used is the one usually employed in the GCM, namely a distribution derived by a two-dimensional chemical model (Brühl 1993) and hereafter called the MAINZ ozone. The data are given as monthly and zonal means from the surface up to 0.18 hPa. Since the top of the ozone distribution is 0.18 hPa, the ozone concentrations between this level and 0.01 hPa are fixed to the value at 0.18 hPa. The second ozone distribution used is an observation-based ozone climatology. It is constructed from ozone sonde profiles (range 1000 - 10 hPa) from 40 stations, which are combined with SUBV-SBUV/2 satellite observations (range 30 - 0.3 hPa) from 1980 to 1991 (Fortuin and Kelder 1998). The ozone concentrations are given as monthly means for 17 zonal bands at 19 pressure levels (1000 - 0.3 hPa). For more information about the KNMI ozone climatology, see Fortuin and Kelder (1998). The KNMI ozone concentrations above 0.3 hPa are fixed to the 0.3 hPa value. Given that both distributions are kept constant in the upper mesosphere, both are somewhat unrealistically there.

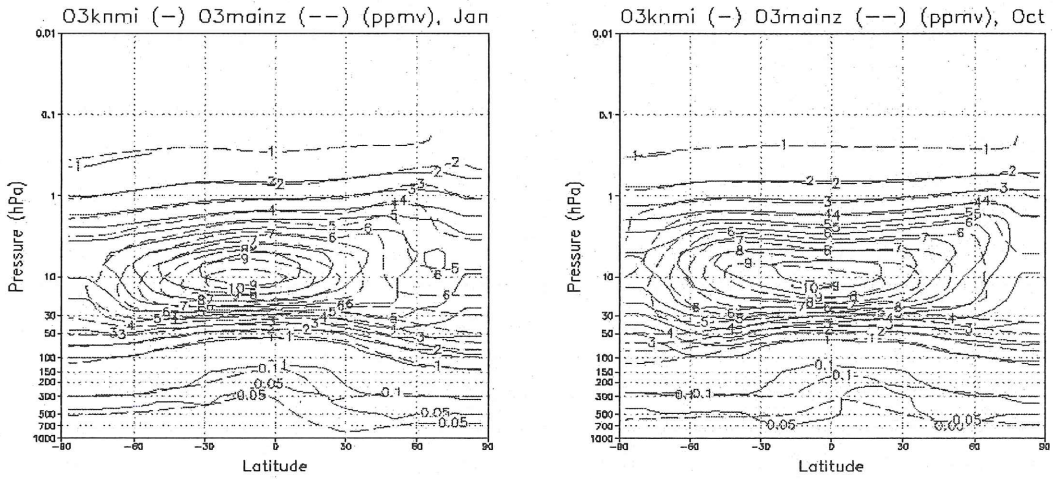


Figure 1: Ozone distributions (ppmv): KNMI (solid line) and MAINZ (dashed line) for January (left) and October (right). Contour levels: 1 ppmv. In addition, 0.05 and 0.1 contours are shown.

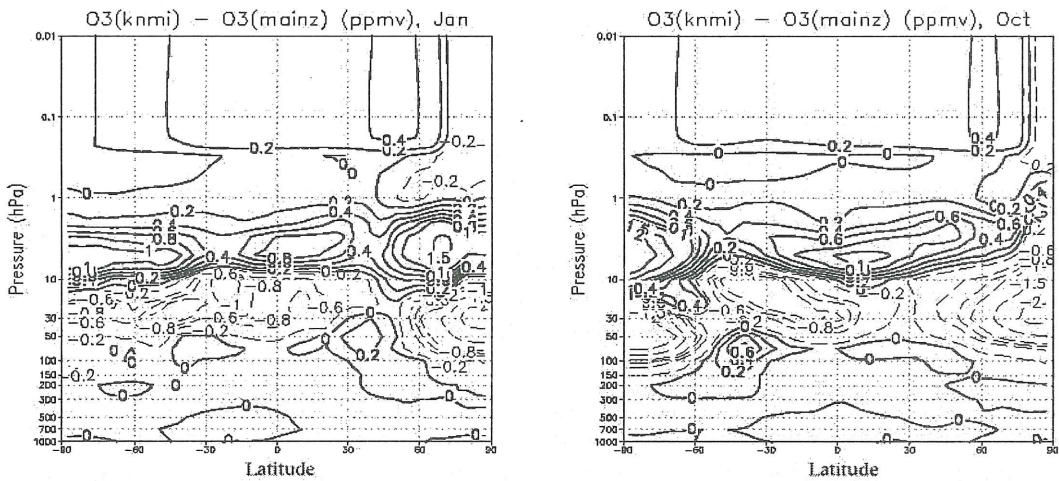


Figure 2: Differences between the ozone distributions (ppmv), KNMI - MAINZ, for January (left) and October (right). Contour levels: 0.2 ppmv between -1 and 1 ppmv, 0.5 otherwise.

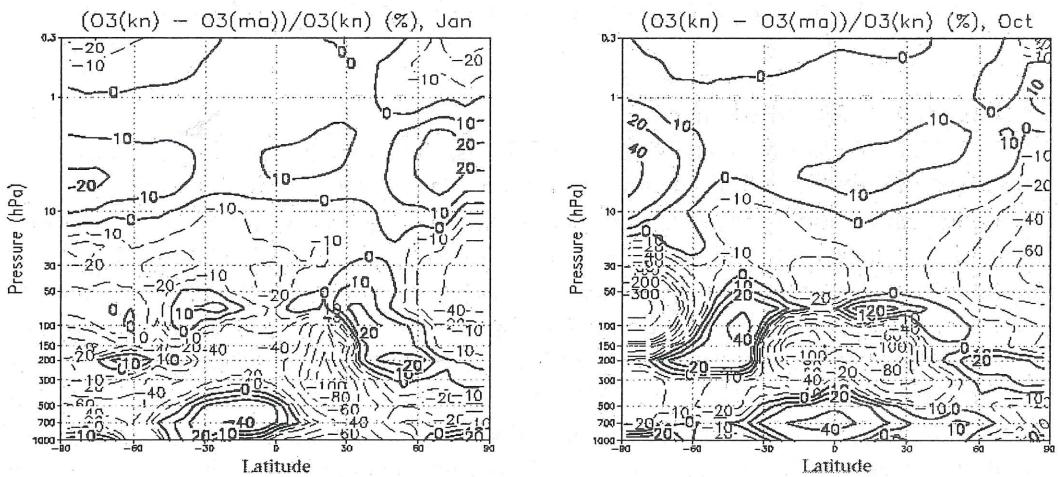


Figure 3: Relative differences between the ozone distributions (%), (KNMI - MAINZ)/KNMI, for January (left) and October (right). Contour is 20% between -100 and +100%, 100% otherwise. In addition, the $\pm 10\%$ isoline is shown.

3.1 Comparison of the two ozone distributions

In Figs. 1, 2 and 3 the KNMI and MAINZ ozone fields are compared for a summer/winter case (represented by January) and an equinox case (represented by October). The largest absolute differences are found where the ozone maximum is located, mainly due to a vertical displacement of the ozone peak (e.g. the MAINZ ozone maximum is located about 5 hPa below the ozone maximum in the KNMI ozone). The maximum in the MAINZ ozone distribution is also 0.8 ppmv higher than the maximum in the KNMI ozone climatology. Although small in absolute sense, the relative differences in the upper troposphere above the tropics reach 100% at some locations.

For January, below 10 hPa, the KNMI ozone climatology has less ozone than the MAINZ ozone distribution with a minimum of 2 ppmv between 100 and 30 hPa over the North Pole. This is up to 40% of the local ozone concentration in the KNMI ozone climatology. Between 10 and 1 hPa the KNMI ozone climatology has between 0 and 1.5 ppmv more ozone than the MAINZ ozone distribution, which is up to 20% at high latitudes of the local KNMI ozone climatology concentrations.

For October, the KNMI ozone climatology includes the ozone hole over the South Pole, whereas the MAINZ ozone distribution does not. This results in an up to 300% lower ozone concentration between about 100 and 50 hPa over the South Pole for the KNMI as compared to the MAINZ ozone distribution. Above the ozone hole, the KNMI ozone distribution has larger concentrations, leading to a relative difference of up to 40%. These differences between the two ozone distributions influence the MAECHAM4 simulations of the temperature and wind distributions as will be shown in the following sections.

In order to evaluate the quality and representativeness of the MAINZ and KNMI ozone distributions for the 1980s, it is interesting to compare them to other published ozone climatologies based on measurements from the same time period. Fortuin and Kelder (1998) compared the KNMI ozone climatology to an ozone climatology compiled at the State University of New York and Albany (SUNYA) (Wang *et al.* 1995). The SUNYA ozone climatology was constructed using TOMS data from 1978-1992, SAGE II data from 1984-1989, and ozone sonde data from 40 stations from 1963 to 1984 (Logan 1985; Spivakovsky 1990). The results from this comparison are here briefly summarized and compared to the differences between the KNMI and the MAINZ ozone distributions as follows: The main differences between the KNMI and SUNYA climatologies occur in the stratosphere. The KNMI ozone concentrations are on the order of 10% lower than the SUNYA ones outside the polar regions at around 10 hPa (the level of the ozone peak). This was also the case when comparing the KNMI ozone climatology to the MAINZ ozone distribution. The accuracy of the SAGE II data is about 7% (McCormick *et al.* 1989), whereas the SBUV-SBUV/2 data should not have systematic errors above 10% (Randel and Wu 1995). The KNMI ozone climatology is therefore, due to the higher uncertainty of the SBUV-SBUV/2 measurements, likely to contain slightly too low ozone maximum concentrations in this region. The differences between the KNMI and SUNYA ozone climatologies increase up to about 0.3 hPa where the SUNYA ozone concentrations are about 50% larger. When comparing the KNMI and MAINZ ozone distributions between 10 and 0.3 hPa and outside the polar regions, the MAINZ ozone concentrations are up to 20% lower than the KNMI ones. The KNMI ozone climatology is assumed more realistic than the MAINZ ozone distribution in this region, based on the comparison with the SAGEII measurements. Another large difference between the KNMI and SUNYA ozone climatologies occurs over the South

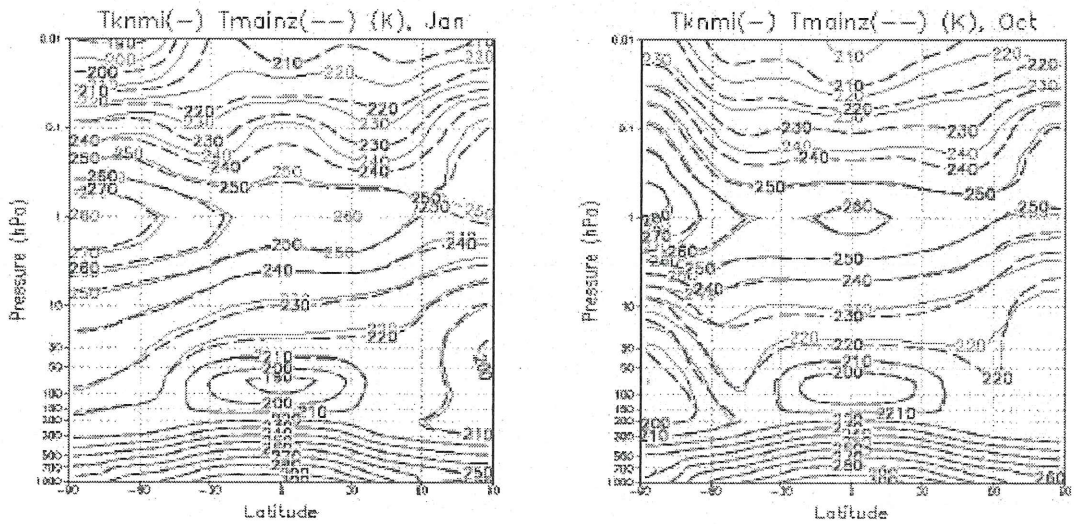


Figure 4: 15 year ensemble averages for January (left) and October (right) of the zonal mean temperature (K): KNMI simulation (solid line) and MAINZ simulation (dashed line). Contour levels: 10 K.

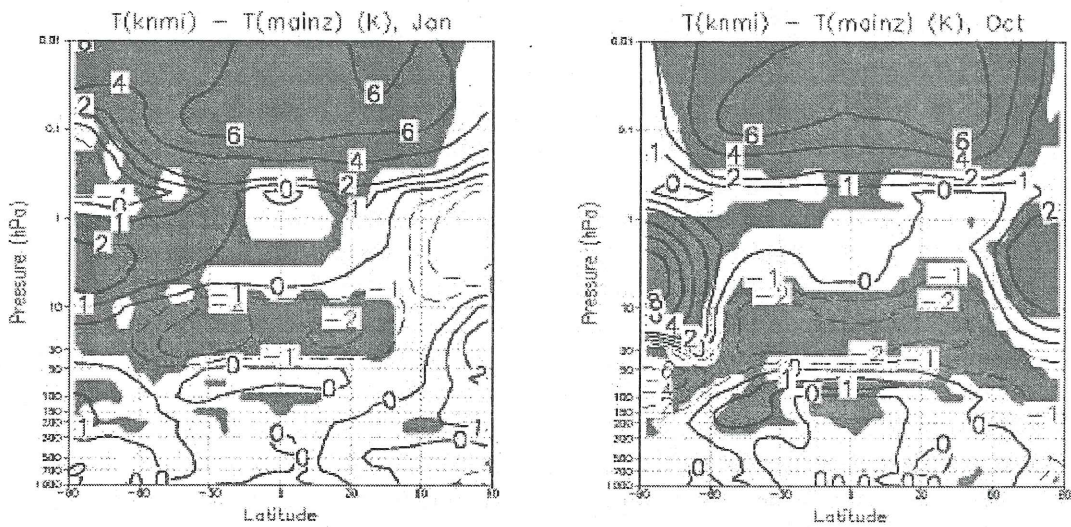


Figure 5: KNMI - MAINZ difference, zonal mean temperature (K) for January (left) and October (right). The shaded areas indicate areas with significant differences within a limit of 98%. Contour levels: 1 K between -2 and 2 K, 2 K otherwise.

Pole. This difference is attributed to the fact that the SUNYA ozone climatology does not contain measurements from the polar regions. In this area the KNMI ozone climatology is, due to its inclusion of ozone sonde measurements, more realistic than the SUNYA. Note that the MAINZ ozone distribution does not represent the ozone hole by construction (Brühl, 1993).

4. Comparison of the climate simulations

Results are presented for 15-year averages from two simulations performed with the MAECHAM4 model, using both ozone distributions. Respectively, the simulation using the KNMI ozone distribution is labeled KNMI, and the one using the MAINZ ozone distribution is labeled MAINZ. The initial fields used are from previous model simulations, and the 15 years considered exclude spin-up time.

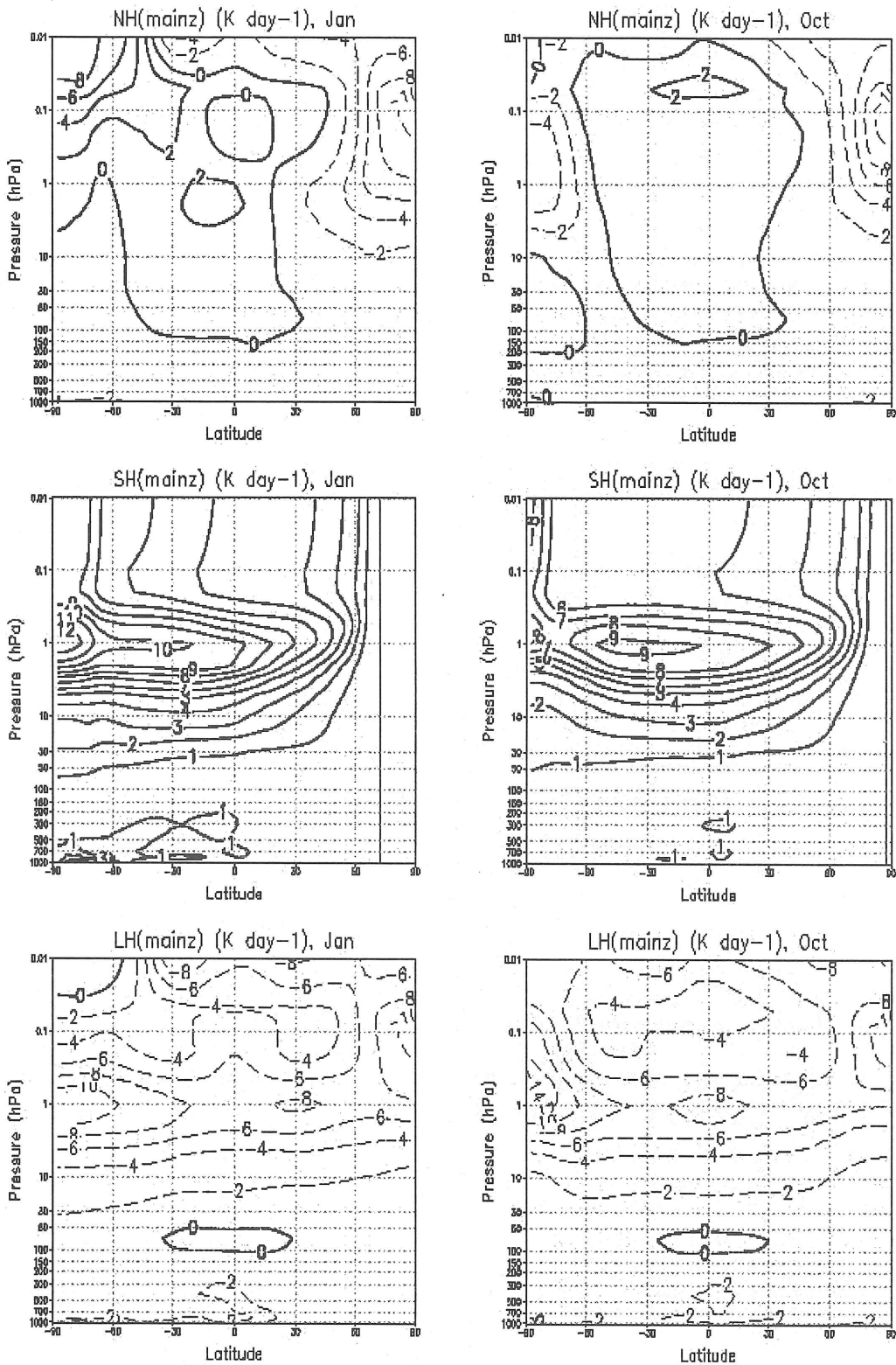


Figure 6: 15-year averages for January (left) and October (right) of the net (upper panel), short wave (middle panel), and long wave (lower panel) heating rates (K/day): MAINZ simulation. Contour levels are 1 K/day for the short wave heating and 2 K/day for the net and long wave heating.

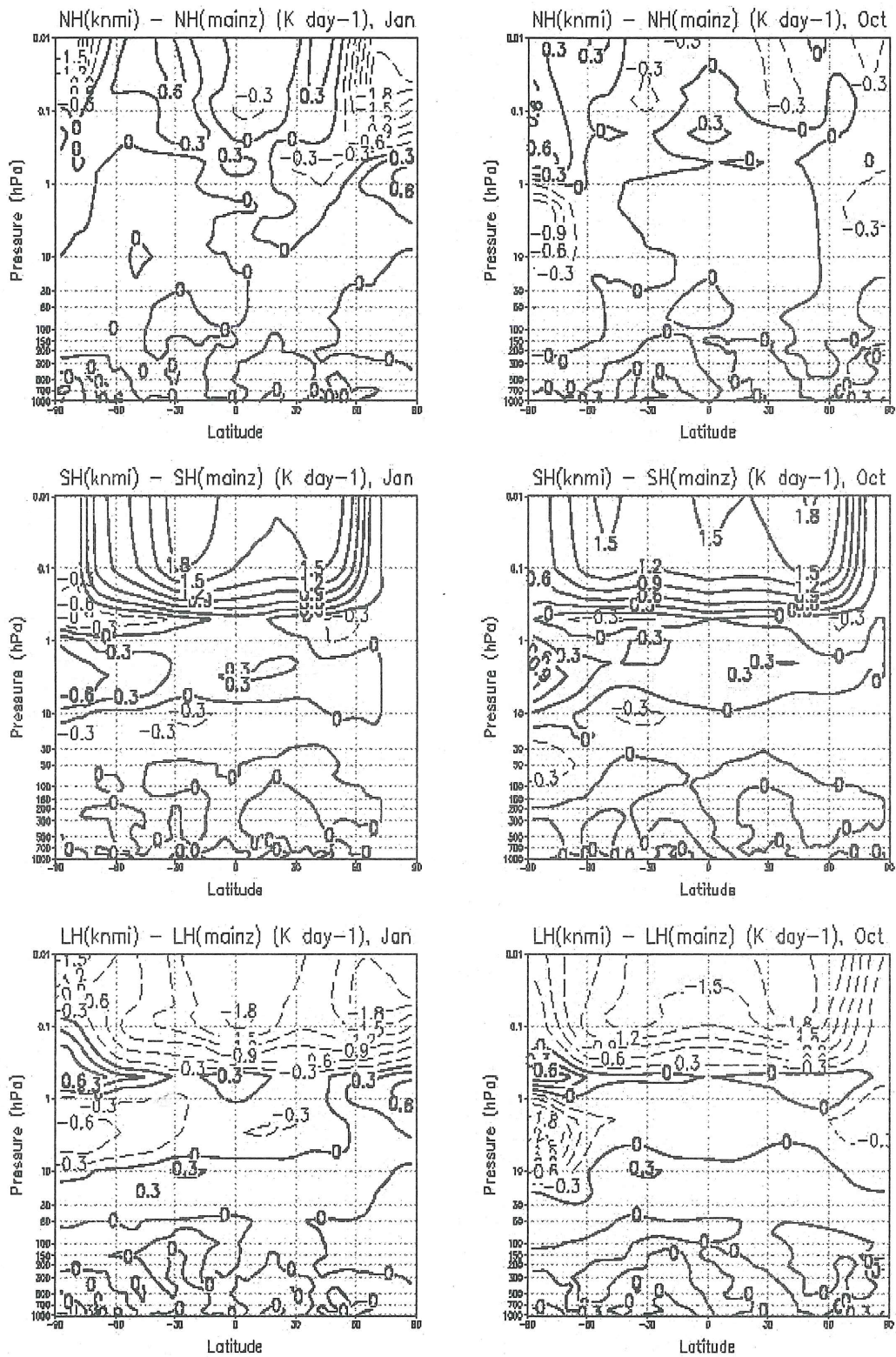


Figure 7: KNMI - MAINZ difference, net, short wave, and long wave heating rates (K/day) for January (left) and October (right). Contour levels: 0.3 K/day.

4.1 Temperatures and Heating Rates

The monthly zonal mean temperatures (15-year averages) from the two MAECHAM4 simulations were compared (Fig. 4) for a summer/winter case (January) and an equinox case (October). Fig. 5 shows the differences in temperature between the two simulations. The shaded areas indicate where the differences are significant at a level of 98% (according to the Student's *t*-test). The respective long wave, short wave, and net heating rates are shown in Figs. 6 and 7.

For January significant differences (KNMI-MAINZ) in temperature are found between 50 and 10 hPa in the tropics (about -2 K). This is in agreement with the lower KNMI ozone concentrations, and consistent with the local decrease in short wave heating rates due to less short wave absorption by ozone (Figs. 6 and 7). Since the temperature is lower for KNMI, the local (negative) long wave heating rates get weaker (a positive difference) (see Figs. 6 and 7). At high southern latitudes (the summer pole) between 10 and 1 hPa, the KNMI temperatures are 2 K warmer. Between 1 and 0.1 hPa they are ~2 K colder. These significant differences are again in agreement with the respective ozone and short/longwave heating rate differences. Also in the mesosphere where the KNMI simulation is ~6 K warmer between ~60°N and S, the significant differences are in agreement with the differences in ozone. The significant temperature differences found for January can therefore be interpreted as a direct radiative response and re-adjustment of the model temperatures to a new radiative equilibrium, leading to small differences in the net heating rate. At polar latitudes and in the mesosphere the differences in the net heating rate are instead somewhat larger, indicating that changes in the circulation have occurred. For instance, above the North Pole between 10 and 0.5 hPa, the negative temperature difference of ~2K is consistent with the decrease in the net cooling rate. However, this difference is not significant because of the large inter-annual variability of the polar night vortex. Above 0.5 hPa the temperature difference turns positive, again in agreement with the increase in cooling rates in the winter northern polar mesosphere. It is further worth noticing that the differences in tropospheric and surface temperatures are very small and, for the greater part, not significant.

For October, the temperature differences between 50 and 10 hPa over the tropics and above 0.3 hPa are also a direct radiative response, as was found for January. Over the South Pole the temperature differences are also in agreement with the local differences in ozone: Between 150 and 30 hPa (where KNMI ozone is lower) the temperatures are up to 6 K lower for KNMI; and between 10 and 1 hPa (where the KNMI ozone is higher) the KNMI temperatures are up to 8 K higher. However, in the latter case the differences in the long wave cooling rate are larger than those in the short wave heating. This leads to a noticeable difference in the net heating rate (Fig. 7), which indicates that a change in the circulation in the model also contributes to the temperature difference. In the Northern Hemisphere, between 10 and 1 hPa at the Pole, the KNMI temperatures are ~2 K higher. Interestingly, this significant difference appears to be dynamically driven, since it is associated with a negative difference in the net heating rates (Fig. 7).

4.2 Zonal Wind

Fig. 8 shows the January and October mean zonal winds (15-year averages) from both simulations, whereas Fig. 9 shows the differences in the zonal wind (KNMI-MAINZ). A general feature valid for both months is that the wind fields are more or less similar in the troposphere, with larger differences occurring in the stratosphere and the mesosphere where the temperature differences are larger (Fig. 5)

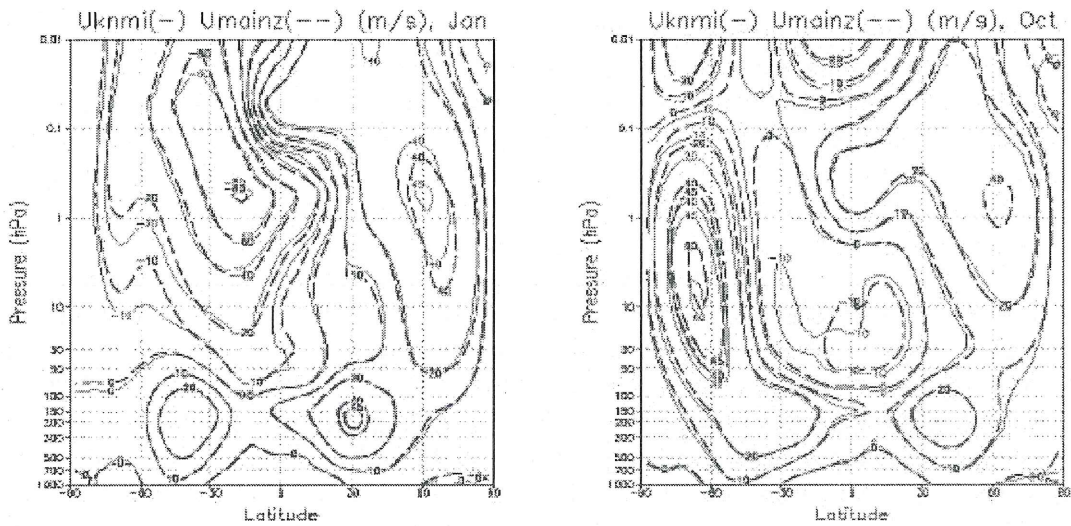


Figure 8: 15-year ensemble averages for January (left) and October (right) of the zonal mean zonal wind (m/s): KNMI simulation (solid line) and MAINZ simulation (dashed line). Contour levels: 10 m/s.

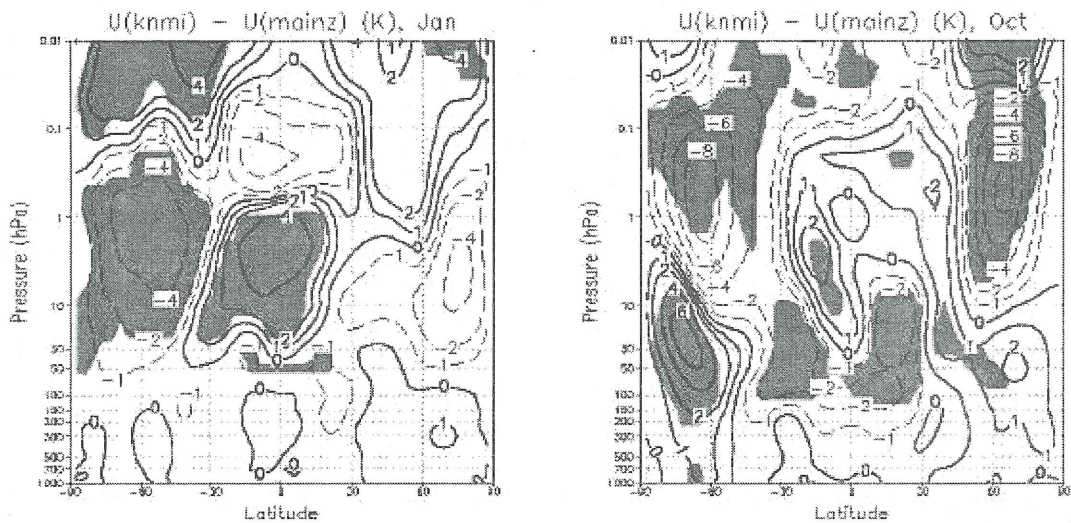


Figure 9: KNMI - MAINZ difference, zonal mean zonal wind (m/s) for January (left) and October (right). The shaded areas indicate areas with significant differences within a limit of 98%. Contours: 1 m/s between -2 and 2 m/s, 2 m/s otherwise.

and the winds stronger (Fig. 8). The wind fields are in most cases of the same order of magnitude, but the jet core locations are slightly horizontally and vertically shifted (Fig. 8).

For January, the significant differences in the wind field occur in the same locations of those in temperature, e.g. in the Southern Hemisphere (summer season) and in the tropical stratosphere. In the Southern Hemisphere between about 10 and 0.5 hPa, the KNMI isotachs are shifted downward with respect to the MAINZ ones (Fig. 8). Therefore the KNMI easterlies are up to 4 m/s stronger. Another significant difference occurs at the same altitude between 30°S and equator (4 m/s weaker easterlies), and poleward of 30°S above 0.1 hPa (2-4 m/s weaker easterlies). The weakening of the easterlies between 30°S and equator and their strengthening poleward of 30°S imply a poleward shift of the stratospheric jet, consistently with the increase in temperature over the South Pole for the KNMI simulation (Fig. 5). In the

mesosphere the situation is reversed: the temperature gradient is stronger in the KNMI simulation and the easterlies decrease more rapidly in magnitude with height.

In October, the differences in the zonal winds are relatively large in both hemispheres. Significant differences (2-6 m/s) occur between about 150 and 10 hPa above the South Pole where the KNMI temperatures are colder. Between about 10 and 0.1 hPa at both southern and northern high latitudes, the westerlies are significantly weaker (2-8 m/s) in the KNMI simulation. This is consistent with the warmer poles and the increased net cooling rates for the KNMI simulation.

4.3 Residual Mean Circulation

The residual mean circulation has been diagnosed from the simulated temperature and the 3 dimensional winds, instantaneous fields saved every 12 hours, following the Transformed Eulerian Mean (TEM) approach described by Andrews *et al.* (1987). It is most clearly illustrated by the streamfunction, shown in Fig. 10 for the 15-year ensemble average for January and October. Fig. 11 shows the differences in the stream function for the same months. In January, the middle atmosphere circulation of both simulations is characterized by a single cell with air ascending in the Southern hemisphere and descending in the Northern hemisphere at polar latitudes. Therefore, the mesospheric air flows from the Southern to the Northern hemisphere. In October (close to the equinox), the circulation is more symmetric with respect to the Equator, with upwelling in the tropics and downwelling at both Southern and Northern polar latitudes (e.g., 2-cell structure).

For January, at Northern polar latitudes, the KNMI circulation is stronger between 100 and about 10 hPa, weaker between about 10 and 0.5 hPa, and again stronger above. This relatively complicated structure is consistent with the difference in net heating rates and in temperature, confirming that such changes are driven by dynamical processes. In the Southern hemisphere the differences in circulation are less coherent in the latitude-altitude section because dynamical processes play a minor role in determining the temperature structure.

For October, both circulation cells are stronger in the KNMI simulation, consistently with the differences in net heating rates, temperatures, and in zonal winds in the upper polar stratosphere of both hemispheres. Given the significance of the differences in temperature and zonal winds, such circulation differences can be interpreted as a consequence of the imposed differences in the ozone fields.

5. Conclusions

Two different ozone distributions have been used in the MAECHAM4 GCM (T30 truncation, L39 vertical levels). This was done to evaluate the model's sensitivity to two different ozone distributions, one used in the standard model and the other to be used in the next model cycle. Both the radiative and dynamic responses of the model to the imposed ozone changes have been diagnosed.

The differences in ozone are largest in the lower stratosphere with 10 to 20% lower ozone concentrations for the KNMI ozone climatology in the tropics and extra-tropics, and between 40 and 300% lower ozone concentrations over the poles. In the upper stratosphere and mesosphere, the ozone concentrations are between 20 and

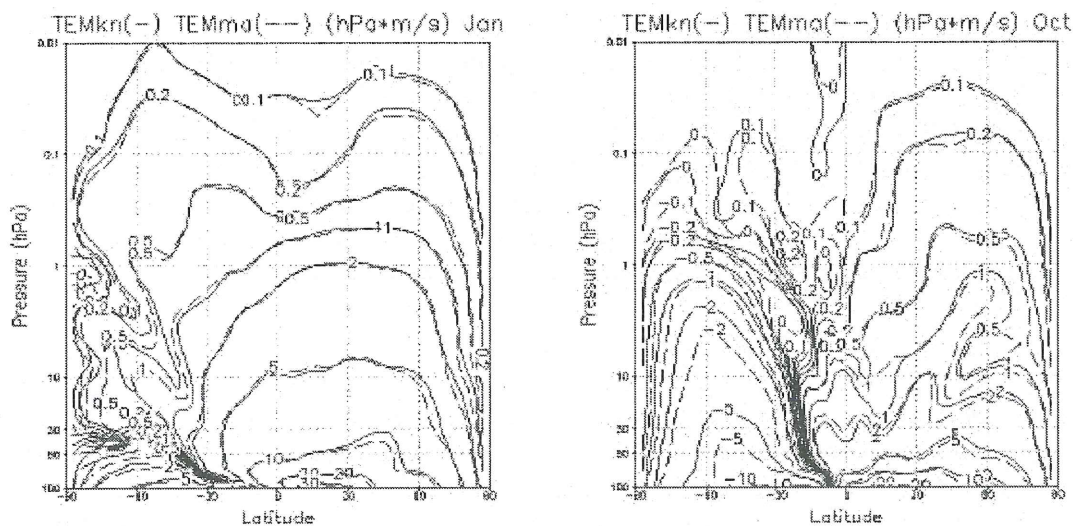


Figure 10: 15-year ensemble averages for January (left) and October (right) of the residual mean streamfunction (hPa m/s): KNMI simulation (solid line) and MAINZ simulation (dashed line). Contour levels: 0, ± 0.1 , ± 0.2 , ± 0.5 , ± 1 , ± 2 , ± 5 , ± 10 , etc.

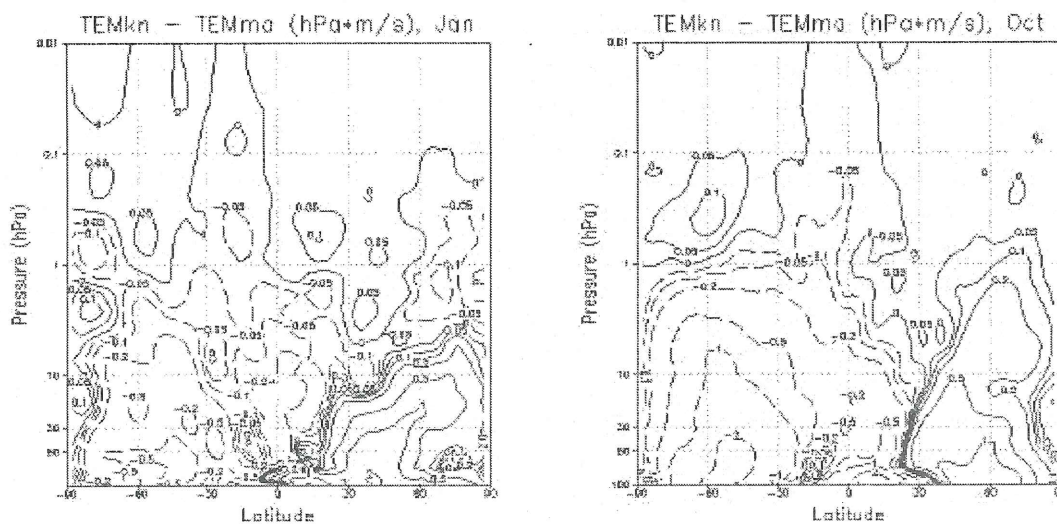


Figure 11: KNMI - MAINZ difference, residual mean streamfunction (hPa m/s) for January (left) and October (right). Contour levels: 0, ± 0.1 , ± 0.2 , ± 0.5 , ± 1 , ± 2 , ± 5 , ± 10 , etc.

40% higher for the KNMI ozone climatology except over the poles in the mesosphere where there is less ozone. The middle atmosphere circulation as simulated by the MAECHAM4 model has shown some sensitivity to the imposed ozone changes. Namely, differences in the stratospheric and mesospheric temperatures on the order of 2 to 8 K have been found. The temperature changes are in most cases consistent with a direct radiative response to the ozone changes except between 10 and 1 hPa above the poles in winter (January), and spring and autumn (October). The latter being instead consistent with changes in the adiabatic heating due to changes in the mean residual circulation. Differences in zonal wind occur in most cases in accordance with thermal wind considerations. Most of the changes are not related to large changes in the strength of the stratospheric jets, but are rather to vertical and horizontal shifts of the wind fields. The local differences are on the order of 2 to 8 m/s.

The temperature and zonal wind differences found here are on the same order of magnitude as the changes found by Christiansen *et al.* (1997) when these are scaled down to match the differences in ozone between the KNMI and MAINZ ozone climatologies. For January, a dynamical cooling of the upper stratosphere over the North Pole is found both by Christiansen *et al.* (1997) and by this study (although not significant in this study), and the cooling is in both cases explained by changes in the meridional and vertical circulation.

Acknowledgements

The authors direct special thanks to Paul Fortuin for his contribution through his work with the compilation of the KNMI ozone climatology. Hennie Kelder and Peter van Velthoven are also thanked for reading and giving comments to this manuscript. Part of this work was funded by the European Union through the project "Study of Indirect and Direct Influences on Climate of Anthropogenic Trace gas Emissions III" (SINDICATE III), project number ENV4-CT97-0483.

References

- Andrews, D. G., J. R. Holton, and C. B. Leovy (1987) Middle atmospheric dynamics, 489 pp., Academic press, San Diego, CA.
- Bintanja, R., Fortuin, J.P.F., and Kelder, H. (1997) Simulation of the Meridionally and Seasonally Varying Climate Response Caused by Changes in Ozone Concentration, *J. Clim.*, **10**, 1288-1311.
- Brühl, C. (1993) Atmospheric effects of stratospheric aircraft. *Rep 1992 Models and Measurements Workshop (Prather M, Remsberg E, eds.)*. NASA Ref Publ. 1292 II.
- Christiansen B., Guldborg, A., Hansen, A.W., Riishøjgaard, L.P. (1997) On the response of a three-dimensional general circulation model to imposed changes in the ozone distribution. *JGR*, **102** (D11), 13,051-13,077.
- Dorland, R. van, and Fortuin, J.P.F. (1994) Simulation of the observed stratospheric temperature trends 1967-1987 over antarctica due to ozone hole deepening. *Proc. of Non-CO2 Greenhouse Gases (NCGG-2) International Symposium*, Noordwijkerhout, The Netherlands, 237-245.
- Forster, P.M.F. and Shine K.P. (1999) Stratospheric water vapor changes as a possible contributor to observed stratospheric cooling. *GRL*, **26** (21), 3309-3312.
- Fortuin, J.P.F. and Kelder, H. (1998) An ozone climatology based on ozonesonde and satellite measurements. *JGR*, **103** (D24), 31,709-31,734.
- Fusco, A.C. and Salby, M.L. (1999) Interannual variations of total ozone and their relationship to variations of planetary wave activity. *J. Clim.*, **12**, 1619-1629.

- Kirk-Davidoff, D.B., Hints, E.J., Anderson, J.G., Keith, D.W. The effect of climate change on ozone depletion through changes in stratospheric water vapor, *Nature*, **402**, 399-401.
- Lacis, A.A., Wuebbles, D.J., and Logan, J.A. (1990) Radiative forcing of climate by changes in the vertical distribution of ozone. *JGR*, **95**, 9971-9982.
- Logan, J.A. (1985) Stratospheric ozone: Seasonal behaviour, trends, and anthropogenic influence, *JGR*, **90**, 10,463-10,482.
- Manzini, E., and McFarlane, N.A. (1998) The effect of varying the source spectrum of a gravity wave parameterization in a middle atmosphere general circulation model, *JGR*, **103**, 31,523-31,539.
- Manzini, E., McFarlane, N.A., and McLandress, C. (1997) Impact of the Doppler spread parameterization on the simulation of the middle atmosphere circulation using the MA/ ECHAM4 general circulation model, *JGR*, **102**, 25,751-25,762.
- McCormick, M.P., Zawodny, J.M., Veiga, R.E., Larsen, J.C., and Wang, P.H. (1989) An overview of SAGE 1 and II ozone measurements, *Planet. Space Sci.*, **37**, 1567-1586.
- Ramanathan, V., Callis, L.B., and Boughner, R.E. (1976) Sensitivity of surface temperature to perturbations in the stratospheric concentrations of ozone and nitrogen dioxide, *J. Atmos. Sci.*, **33**, 1092-1112.
- Ramaswamy, V., Schwarzkopf, M.D., and Randel, W.J. (1996) Fingerprint of ozone depletion in the spatial. and temporal pattern of recent lower-stratospheric cooling. *Lett. Nature*, **382**, 616-618.
- Randel, W.J. and Cobb, J.B. (1994) Coherent variations of monthly mean total ozone and lower stratospheric temperature. *JGR*, **99** (D3), 5433-5447.
- Randel, J.W., and Wu, F. (1995) Climatology of stratospheric ozone based on SBUV and SBUV/2 data: 1978-1994, *NCAR Techn. Note 412+STR*, NCAR, Boulder Colo., 137 pp.
- Roeckner, E., Arpe, K., Bengtsson, L., Christoph, M., Claussen, M., Dümenil, L., Esch, M., Giorgetta, M., Schlese, U., and Schulzweida, U. (1996) The atmospheric general circulation model ECHAM4: Model description and simulation of present day climate, *MPI Rep.*, **218**, 90 pp., Hamburg, Germany.
- Solomon (1999) Stratospheric ozone depletion: A review of concepts and history. *Rev. of Geophys.*, **37** (3), 275-316.
- Spivakovsky, C.M., Yevich, R., Logan, J.A., Wofsy, S.C., McElroy, M.B., and Prather, M.J. (1990) Tropospheric OH in a three-dimensional chemical model: An assessment based on observations of CH₃CCL₃, *JGR*, **95**, 18,441-18,471.

Straume, A.G., Fortuin, J.P.J., Siegmund, P., Kelder, H., Roeckner, E. (1999) Modelling the effects of ozone changes on climate. *Proc. of Non-CO2 Greenhouse Gases (NCGG-2) International Symposium*, Noordwijkerhout, The Netherlands.

Thompson, D.W.J. and Wallace, J.M. (1998) The Arctic Oscillation signature in the wintertime geopotential height temperature fields. *GRL*, **25** (9), 1297-1300.

Wang, W.-C., Liang, X.-Z., Dudek, M.P., Pollard, D., and Thompson, S.L. (1995) Atmospheric ozone as a climate gas., *Atmos. Research*, **37**, 247-256.

Wang, W. -C., Pinto, J.P., and Yung, Y.L. (1980) Climate effects due to halogenated compounds in the earth's atmosphere. *J. Atmos. Sci.*, **37**, 333-338.

WMO (1999) Scientific Assessment of Ozone Depletion: 1998, Report No. 44, World Meteorological Organization, Geneva, Switzerland.

Eerder gepubliceerde titels in de reeks *Intern Rapport*:

- 2000-01 Inventarisatie nowcasting-technieken voor gevaarlijk weer : eindrapport
G.T. Geertsema, A. Maas, H.R.A. Wessels, H. Benschop, B. Blaauboer en C.J. Kok
- 2000-02 COST-76 : aims, achievements and future
W.A. Monna
- 2000-03 Verslag van een studiereis naar de National Weather Service van de USA, juni 2000
A.W. Donker
- 2000-04 Definitiestudie vervanging IBDS : eindrapport
Sylvia Barlag, Hans Roozkrans, Richard Rothe, Jan Bijma, Jan Jans en Frans Debie
- 2000-05 Rapportage voorstudie herinrichting Cabauw
Projectgroep Voorstudie Herinrichting Cabauw
- 2001-01 Neerslagonderzoek
Foeke Kuik
- 2001-02 Estimation of the maximum velocity of convective wind gusts
Iwan Holleman
- 2001-03 Synoptisch Waarneemnet Nederland 2000 (SWaNet NL 2000)
J.P. van der Meulen
- 2001-04 Eindrapport AutoTrend "Automatische generatie TREND 'S"
Albert Jacobs
- 2002-01 Sensitivity of the MAECHAM4 model to imposed ozone distributions
Anne Grete Straume, Elisa Manzini and Peter Siegmund

